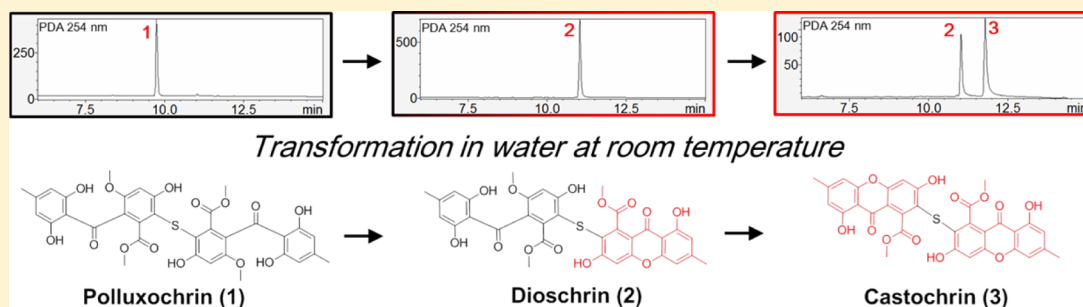


Bioactive Sulfur-Containing Sulochrin Dimers and Other Metabolites from an *Alternaria* sp. Isolate from a Hawaiian Soil Sample

Shengxin Cai,^{†,‡} Jarrod B. King,^{†,‡} Lin Du,^{†,‡} Douglas R. Powell,[‡] and Robert H. Cichewicz^{*,†,‡}

[†]Natural Products Discovery Group, Institute for Natural Products Applications and Research Technologies, and [‡]Department of Chemistry and Biochemistry, Stephenson Life Sciences Research Center, 101 Stephenson Parkway, University of Oklahoma, Norman, Oklahoma 73019-5251, United States

S Supporting Information



ABSTRACT: Polluxochrin (1) and dioschirin (2), two new dimers of sulochrin linked by thioether bonds, were purified from an *Alternaria* sp. isolate obtained from a Hawaiian soil sample. The structures of the two metabolites were established by NMR, mass spectrometry data, and X-ray analysis. Metabolite 1 was determined to be susceptible to intramolecular cyclization under aqueous conditions, resulting in the generation of 2 as well as another dimeric compound, castochrin (3). An additional nine new metabolites were also obtained, including four new pyrenochaetic acid derivatives (8–11), one new asterric acid analogue (13), and four new secalonin acid analogues (14–17). Bioassay analysis of these compounds revealed 1–3 displayed antimicrobial and weak cytotoxic activities.

The Hawaiian Islands consist of a patchwork of biodiverse habitats exhibiting a high degree of species endemism.^{1,2} Recent reports in the field of natural products have highlighted the impact of Hawaii's biodiversity on the likelihood for discovering new bioactive metabolites, especially from microbial sources.^{3–7} For example, our research group reported the discovery of several new bioactive metabolites from a biosynthetically talented fungal (*Aspergillus* sp.) isolate obtained from soil collected near Waikiki Beach, Honolulu, Hawaii.⁸ Among the compounds obtained from this fungus, the new prenylated indole alkaloid waikialoid A was notable because of the potent inhibition it afforded against *Candida albicans* biofilm formation (IC₅₀ 1.4 μM).⁸

An examination of additional samples from the Hawaiian Islands has provided a second biosynthetically talented fungal isolate, Wailua PDA-3, from a soil sample collected in the vicinity of Wailua Falls. An ethyl acetate extract prepared from a small-scale solid-phase fermentation of this fungus exhibited antifungal activity against both *C. albicans* and *Aspergillus fumigatus*. Subsequent LC-PDA-ESIMS profiling of the isolate's secondary metabolome revealed an assortment of chemically diverse metabolites with masses ranging from approximately 200 to 700 Da. Sequencing of the isolate's ITS region suggested that the fungus was taxonomically similar to *Alternaria longissima*. LC-PDA-ESIMS-based dereplication of natural products reported from this genus revealed that none of the

putative metabolites we observed could be readily attributed to those ascribed to an *Alternaria* sp.

In this report, we describe 12 new natural products from this *Alternaria* sp. isolate. All of the compounds were tested in bioassays targeting different cell types and bioactivity end points (including antibacterial, antifungal, cancer cell cytotoxicity, and disruption of *Candida* biofilm formation). Compounds 1–3, which are new sulochrin dimers linked via a thioether bridge, showed antimicrobial and weak cytotoxic activities.

RESULTS AND DISCUSSION

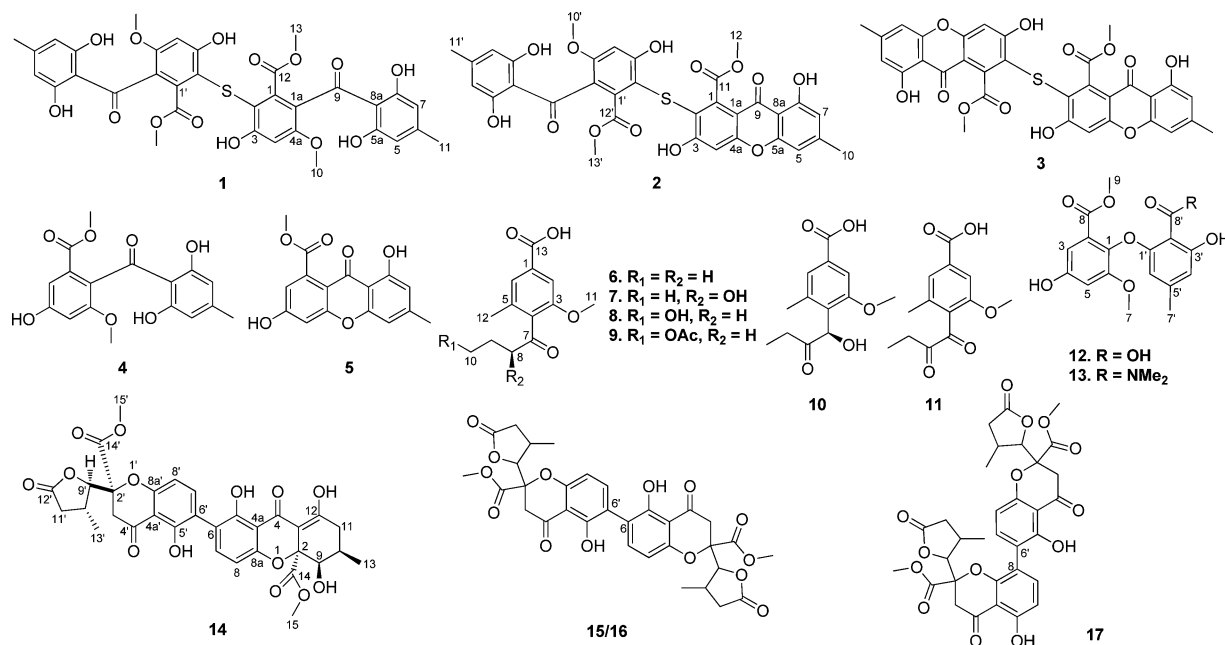
The *Alternaria* sp. isolate was prepared for scale-up chemical analysis by culturing it for 4 weeks on a solid-state medium composed of Cheerios breakfast cereal supplemented with a 0.3% sucrose solution.^{9–11} The fungal biomass was extracted with EtOAc, yielding a crude extract that was subsequently processed over several types of sorbents (including silica gel, Sephadex LH20, and C₁₈) to provide purified metabolites 1–17.

Compound 1 was obtained as a pale yellow, amorphous powder, and its molecular formula was established as

Received: July 4, 2014

Published: September 29, 2014

Chart 1



$C_{34}H_{30}O_{14}S$ based on HRESIMS data ($[M + Na]^+$ ion at m/z 717.1253, calcd 717.1248) indicating 20 degrees of unsaturation. The 1H and ^{13}C NMR spectra of **1** provided evidence for approximately half of the expected proton and carbon resonances, which were assigned as belonging to 11 non-protonated carbons, three methines, three methyls, and three exchangeable protons. The initial analysis of the data set led us to suspect that **1** might be a dimeric compound. Further examination of the 1H and ^{13}C NMR data (Table 1) indicated that the resonances observed for **1** were similar to those for the known metabolite sulochrin (**4**),¹² which we also purified from the same fungal extract. The major differences between **1** and **4** as revealed by NMR were the loss of signals for a methine unit

(δ_H 6.91; δ_C 107.6) and the gain of a new nonprotonated sp^2 carbon resonance (δ_C 109.1). The necessity of including a sulfur atom in **1** as required by the molecular formula led us to propose that the sulfur served as a thioether bridge linking the C-2 and C-2' carbons. Thus, the structure of the new sulochrin dimer was proposed as illustrated (**1**), and the metabolite was given the trivial name polluxochrin. Metabolite **1** shares structural similarities to other sulochrin dimers including, disulochrin,⁹ as well as guignasulfide,¹³ which is a demethoxy analogue of **1**.

Compound **2** was purified as pale yellow, block-like crystals. HRESIMS provided a pseudomolecular ion at m/z 685.0981 $[M + Na]^+$ (calcd 685.0986) that supported the molecular formula $C_{33}H_{26}O_{13}S$. This corresponded to 21 degrees of unsaturation. Inspection of the 1H and ^{13}C NMR data for **2** revealed that the spectra superficially appeared as the superimposition of two sets of signals (Table 2) with one set virtually identical to those generated for compound **1** and the other set bearing substantial similarity to methyl-(1,6-dihydroxy-3-methylxanthone)-8-carboxylate (**5**),¹⁴ which was also purified from the fungal extract. The additional unit of unsaturation afforded via the incorporation of **5** in this metabolite readily accounted for the overall difference of one unsaturation unit between metabolites **1** and **2**. The change from a single C-9 diaryl ketone signal in **1** (δ_C 197.8) (Table 1) to pyrone (δ_C 179.2) and diaryl (δ_C 197.7) ketone signals in **2** (Table 2) further supported the asymmetric dimeric nature of the new metabolite. This assertion was subsequently confirmed by HSQC and HMBC experiments (Figures S9 and S10), as well as data generated from a single-crystal X-ray diffraction experiment (Figure 1). Compound **2** has been given the trivial name dioschirin.

Compounds **1** and **2** were determined to be susceptible to transformation under aqueous conditions. Upon incubation for 48 h in various aqueous solvent mixtures, compound **1** was observed by LC-PDA-ESIMS to transform into **2**, which subsequently converted to another compound (**3**) (Figure S1). The transformation process was determined to be temperature

Table 1. 1H (400 MHz) and ^{13}C (100 MHz) NMR and HMBC Data for Compound **1** (DMSO- d_6)

no.	δ_C , mult.	δ_H , mult.	HMBC
1/1'	136.2 C		
2/2'	109.1 C		
3/3'	160.4 C		
4/4'	100.9 CH	6.52 s	2/2', 3/3', 1a/1a', 4a/4a'
4a/4a'	157.7 C		
1a/1a'	124.3 C		
5/5'	107.9 CH	6.10 s	7/7', 11/11', 8a/8a'
5a/5a'	161.9 C		
6/6'	148.3 C		
7/7'	107.9 CH	6.10 s	5/5', 11/11', 8a/8a'
8/8'	161.9 C		
8a/8a'	109.6 C		
9/9'	197.8 C		
10/10'	56.3 CH ₃	3.61 s	4a/4a'
11/11'	22.1 CH ₃	2.16 s	5/5', 6/6', 7/7'
12/12'	167.3 C		
13/13'	52.3 CH ₃	3.48 s	12/12'
3/3'-OH		10.3 br s	
8/8'-OH		11.2 s	7/7', 8/8', 8a/8a'
5a/5a'-OH		11.2 s	5/5', 5a/5a', 8a/8a'

Table 2. ^1H (400 MHz) and ^{13}C (100 MHz) NMR and HMBC Data for Compound 2 (DMSO- d_6)

no.	δ_{C} , mult.	δ_{H} , mult.	HMBC	no.	δ_{C} , mult.	δ_{H} , mult.	HMBC
1	137.0 C			1'	136.2 C		
2	109.6 C			2'	107.9 C		
3	164.9 C			3'	159.9 C		
4	102.8 CH	6.80 s	2, 3, 1a, 4a	4'	100.8 CH	6.50 s	2', 3', 1a', 4a'
4a	157.2 C			4a'	157.5 C		
1a	118.5 C			1a'	124.4 C		
5	107.8 CH	6.84 s	7, 10, 5a, 8a	5'	107.9 CH	6.11 s	7', 11', 8a'
5a	155.4 C			5a'	161.9 C		
6	149.1 C			6'	148.3 C		
7	111.7 CH	6.63 s	5, 8, 10, 8a	7'	107.9 CH	6.11 s	5', 11', 8a'
8	161.0 C			8'	161.9 C		
8a	106.1 C			8a'	109.6 C		
9	179.2 C			9'	197.7 C		
10	22.4 CH ₃	2.38 s	5, 6, 7	10'	56.3 CH ₃	3.62 s	4a'
11	167.4 C			11'	22.1 CH ₃	2.17 s	5', 6', 7'
12	53.0 CH ₃	3.88 s	11	12'	166.8 C		
8-OH		12.3 br s	7, 8, 8a	13'	52.2 CH ₃	3.48 s	12'
				8'-OH		11.2 s	7', 8', 8a'
				5a'-OH		11.2 s	5', 5a', 8a'

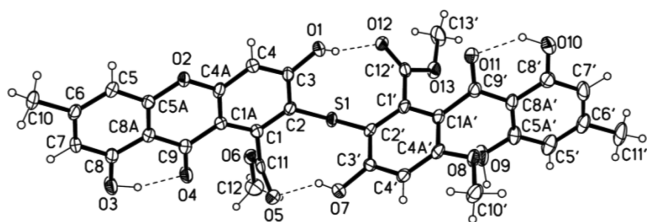
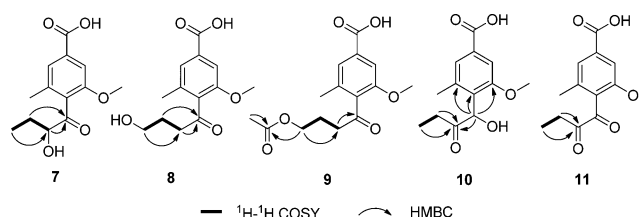


Figure 1. ORTEP structure generated from the X-ray diffraction data for a single crystal of 2.

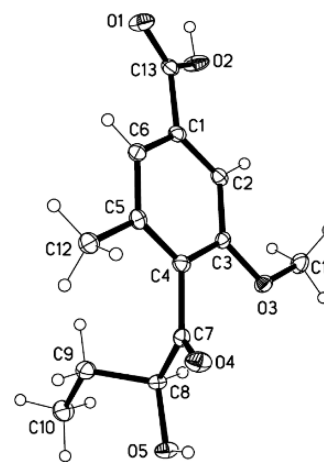
dependent, and even mild heating for brief periods led to the rapid loss of **1** and generation of **2** and **3**. To obtain material for structure characterization, 5.0 mg of **1** in aqueous MeOH was held at 40 °C for 6 h, generating 3.5 mg of **3**. The purified product was examined by HRESIMS, which yielded a pseudomolecular ion at m/z 629.0757 $[\text{M} - \text{H}]^-$ (calcd 629.0754) corresponding to the molecular formula $\text{C}_{32}\text{H}_{22}\text{O}_{12}\text{S}$. An analysis of the ^1H and ^{13}C NMR data for the product (Table S1) indicated that **3** was structurally similar to compounds **1** and **2**. Immediately apparent was that the ^{13}C NMR diaryl ketone signal in **1** (C-9/9', δ_{C} 197.8) had been replaced by a pyrone ketone signal in **3** (C-9/9', δ_{C} 179.1) (Tables 1 and S1). Subsequent 2D NMR experiments (Figures S14 and S15) confirmed that these changes resulted in the formation of a new compound that consisted of a thioether-linked dimer of **5** connected to the sulfur atom through C-2 and C-2'. In contrast to metabolite **1**, compound **3** exhibited two nearly superimposable sets of NMR signals. The doubling of the signals is proposed to result from the hindered rotation of the S–C-2 and/or S–C-2' bonds. Compound **3** has been given the trivial name castochrin. A similar cyclization phenomenon has been observed for the transformation of metabolite **4** to **5**, but in this case, the reaction rate was much slower, taking upward of a week to occur. These results imply that the sulfur atom might serve to accelerate the intramolecular cyclization of **1** into **2** and **3**.

The molecular formula for compound **7** was determined by HRESIMS to be $\text{C}_{13}\text{H}_{16}\text{O}_5$. An analysis of the 1D and 2D NMR (in acetone- d_6 and DMSO- d_6) for **7** indicated that this

metabolite had the same planar structure as pyrenochaetic acid **D**,¹⁵ but the published account of this metabolite did not address the compound's absolute configuration. To address this problem, we prepared crystals of **7** for X-ray diffraction analysis (Figure 3). The metabolite's absolute configuration was

Figure 2. Selected ^1H – ^1H COSY and HMBC correlations for compounds **7**–**11**.

determined to be 8S by the Hooft method.¹⁶ This was further supported by comparing the ECD experimental data for **7** with a computationally derived theoretical spectrum (Figure 4A,

Figure 3. ORTEP structure generated from the X-ray diffraction data for a single crystal of **7**.

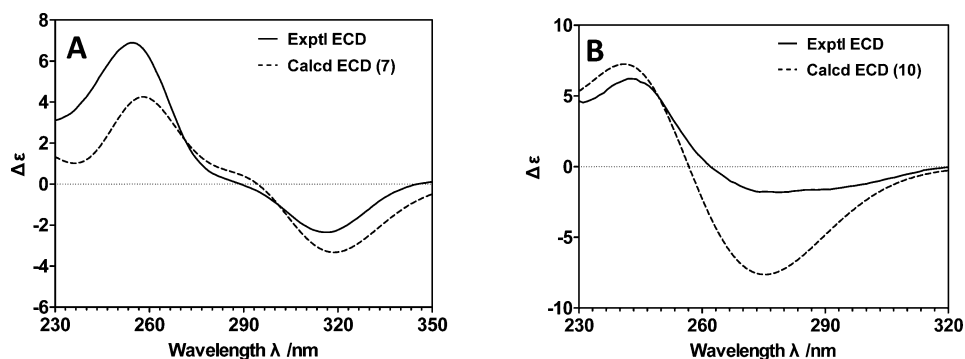


Figure 4. Calculated and experimental ECD data for compounds 7 (A) and 10 (B).

refer to the Supporting Information for a discussion of how the theoretical ECD data for 7 were prepared).

Compound 8 was determined by HRESIMS to have the same molecular formula as 7. Analysis of the ^1H and ^{13}C NMR data for 8 (Tables 3 and 4) revealed that it possessed the same

Table 3. ^1H NMR Data for Compounds 7–11 (400 MHz, $\text{DMSO}-d_6$)

no.	7 δ_{H} , mult. (J in Hz)	8 δ_{H} , mult. (J in Hz)	9 δ_{H} , mult. (J in Hz)	10 δ_{H} , mult. (J in Hz)	11 δ_{H} , mult. (J in Hz)
2	7.36 s	7.39 s	7.40 s	7.31 s	7.42 s
6	7.42 s	7.44 s	7.43 s	7.38 s	7.49 s
7				5.31 s	
8	4.25 dd (8.6, 3.9)	2.76 t (7.4)	2.81 t (5.7)		
9	1.67 m	1.72 m	1.89 m	2.58 dq (18.0, 7.3)	2.82 q (7.2)
	1.45 m			2.31 dq (18.0, 7.3)	
10	0.90 t (7.4)	3.42 t (7.4)	4.03 t (5.4)	0.91 t (7.3)	1.06 t (7.2)
11	3.79 s	3.83 s	3.82 s	3.73 s	3.78 s
12	2.15 s	2.16 s	2.15 s	2.29 s	2.29 s
15			2.00 s		
7-OH				5.52 br s	
13-OH	11.43 br s				13.32 br s

carbon skeleton as the co-occurring metabolite pyrenochaetic acid C (6).¹⁷ However, the carbon and proton signals attributable to an oxidized methylene (CH_2 -10, δ_{H} 3.42; δ_{C} 60.4) were replaced by signals for an aliphatic methyl. Taking into account the HRESIMS data, it was proposed that compound 8 contained a new C-10 hydroxyl group relative to 6. Combining the proton and carbon chemical shift patterns for 8 with the ^1H – ^1H COSY correlations among H-8 and H-9 and H-10, as well as the HMBC correlations between H-8 and H-9 with C-7 (Figure 2), the position of the new hydroxyl group was unambiguously assigned. This new metabolite has been given the name pyrenochaetic acid E (8).

Pyrenochaetic acid F (9) was purified as a colorless, amorphous solid, and its molecular formula was established to be $\text{C}_{15}\text{H}_{18}\text{O}_6$ based on HRESIMS data ($[\text{M} - \text{H}]^-$ ion at m/z 293.1034, calcd 293.1031). The compound exhibited NMR resonances similar to 8 with the addition of proton and carbon signals corresponding to an acetoxy group (Tables 3 and 4). The inclusion of the acetoxy group in the structure was confirmed on the basis of an HMBC correlation from H-10 (δ_{H} 4.03) to C-14 (δ_{C} 170.8) (Figure 2).

Pyrenochaetic acid G (10) was obtained as a colorless, amorphous solid. An $[\text{M} - \text{H}]^-$ molecular ion at m/z 251.0932 (calcd 251.0925) in the HRESIMS spectrum was in agreement with the molecular formula $\text{C}_{13}\text{H}_{16}\text{O}_5$. Compound 10 displayed ^{13}C NMR resonances that were similar to those for 7. The HMBC correlation data (H-7 to C-3, C-4, C-5, and C-8, as well

Table 4. ^{13}C NMR Data for Compounds 7–11 (100 MHz, $\text{DMSO}-d_6$)

no.	7 δ_{C} , mult.	8 δ_{C} , mult.	9 δ_{C} , mult.	10 δ_{C} , mult.	11 δ_{C} , mult.
1	133.1 C	132.7 C	not detected	131.7 C	135.3 C
2	109.5 CH	109.7 CH	109.8 CH	109.9 CH	110.3 CH
3	156.4 C	156.0 C	156.0 C	157.4 C	159.3 C
4	133.6 C	135.2 C	134.0 C	132.7 C	127.9 C
5	136.3 C	135.2 C	134.9 C	139.1 C	140.1 C
6	124.1 CH	124.2 CH	124.2 CH	124.5 CH	124.8 CH
7	209.5 C	207.1 C	206.6 C	72.5 CH	196.3 C
8	78.0 CH	40.8 CH_2	40.5 CH_2	211.9 C	201.7 C
9	26.0 CH_2	26.9 CH_2	22.7 CH_2	31.1 CH_2	29.7 CH_2
10	10.7 CH_3	60.4 CH_2	63.5 CH_2	8.0 CH_3	7.3 CH_3
11	56.2 CH_3	56.3 CH_3	56.2 CH_3	56.2 CH_3	56.8 CH_3
12	19.1 CH_3	18.7 CH_3	18.8 CH_3	19.7 CH_3	19.5 CH_3
13	167.4 C	167.3 C	167.9 C	167.5 C	166.9 C
14			170.8 C		
15			21.1 CH_3		

Table 5. ¹H (400 MHz) and ¹³C (100 MHz) NMR and HMBC Data for Compound 13 (DMSO-*d*₆)

no.	δ _C , mult.	δ _H , mult.	HMBC	no.	δ _C , mult.	δ _H , mult.	HMBC
1	134.2 C			1'	156.1 C		
2	126.5 C			2'	111.4 C		
3	107.6 CH	6.71 s	1, 4, 5, 8	3'	154.7 C		
4	155.4 C			4'	109.6 CH	6.25 s	2', 3', 6', 7'
5	105.3 CH	6.71 s	1, 3, 6	5'	138.9 C		
6	153.7 C			6'	104.3 CH	5.57 s	1', 2', 4', 7'
7	56.5 CH ₃	3.62 s	6	7'	21.7 CH ₃	2.02 s	4', 5', 6'
8	165.6 C			8'	166.2 C		
9	52.5 CH ₃	3.62 s	8	9'	34.3 CH ₃	2.91 s	8', 10'
4-OH		9.47 br s		10'	37.5 CH ₃	2.85 s	8', 9'
				3'-OH		9.81 br s	

Table 6. ¹H (400 MHz) and ¹³C (100 MHz) NMR Data for Compounds 14–17 (DMSO-*d*₆)

no.	14		15		16		17	
	δ _C , mult.	δ _H , mult. (<i>J</i> in Hz)	δ _C , mult.	δ _H , mult. (<i>J</i> in Hz)	δ _C , mult.	δ _H , mult. (<i>J</i> in Hz)	δ _C , mult.	δ _H , mult. (<i>J</i> in Hz)
2	85.3 C		84.9 C		84.1 C		84.6 C	
3	101.0 C		39.3 CH ₂	3.60 d (17.2) 3.11 d (17.2)	39.3 CH ₂	3.58 d (17.2) 3.08 d (17.2)	40.4 CH ₂	3.53 d (17.3) 3.03 d (17.3)
4	187.4 C		196.1 C		196.2 C		196.0 C	
4a	106.5 C		107.5 C		107.3 C		107.6 C	
5	158.9 C		158.7 C		158.6 C		160.8 C	
6	118.1 C		117.5 C		117.4 C		109.9 CH	6.58 d (8.6)
7	140.3 CH	7.39 d (8.5)	141.0 CH	7.49 d (8.5)	141.1 CH	7.47 d (8.6)	141.1 CH	7.47 d (8.6)
8	107.9 CH	6.55 d (8.5)	107.7 CH	6.67 d (8.5)	107.6 CH	6.65 d (8.6)	115.4 C	
8a	157.8 C		159.1 C		158.8 C		156.2 C	
9	70.4 CH	3.95 br s	87.0 CH	4.60 d (4.0)	86.1 CH	4.55 d (5.1)	85.8 CH	4.42 d (4.0)
10	28.8 CH	1.91 m	29.8 CH	2.89 m	29.8 CH	2.89 m	29.6 CH	2.42 m
11	33.0 CH ₂	2.35 m	36.1 CH ₂	2.87 dd (21.6, 9.1) 2.28 dd (21.6, 9.1)	36.2 CH ₂	2.89 dd (17.6, 9.3) 2.31 dd (17.6, 6.0)	35.5 CH ₂	2.13 dd (18.0, 8.9) 2.05 dd (18.0, 5.4)
12	180.5 C		176.1 C		175.8 C		175.9 C	
13	17.8 CH ₃	1.00 d (6.6)	20.3 CH ₃	1.17 d (6.5)	19.7 CH ₃	1.09 d (6.8)	20.2 CH ₃	0.97 d (7.0)
14	171.8 C		169.3 C		169.2 C		169.1 C	
15	53.9 CH ₃	3.64 s	53.9 CH ₃	3.70 s	54.1 CH ₃	3.71 s	54.1 CH ₃	3.68 s
5-OH		11.67 s		11.82 s		11.79 s		11.53 s
9-OH		5.80 br s						
12-OH		13.8 br s						
2'	84.8 C		84.9 C		84.9 C		85.0 C	
3'	39.4 CH ₂	3.58 d (17.2) 3.09 d (17.2)	39.3 CH ₂	3.60 d (17.2) 3.11 d (17.2)	39.3 CH ₂	3.59 d (17.2) 3.09 d (17.2)	39.3 CH ₂	3.60 d (17.2) 3.12 d (17.2)
4'	196.1 C		196.1 C		196.1 C		196.2 C	
4a'	107.4 C		107.5 C		107.5 C		107.5 C	
5'	158.6 C		158.7 C		158.6 C		158.6 C	
6'	117.7 C		117.5 C		117.5 C		117.3 C	
7'	141.2 CH	7.48 d (8.6)	141.0 CH	7.49 d (8.5)	141.0 CH	7.47 d (8.6)	140.9 CH	7.57 d (8.6)
8'	107.6 CH	6.64 d (8.6)	107.7 CH	6.67 d (8.5)	107.7 CH	6.67 d (8.6)	107.7 CH	6.67 d (8.6)
8a'	159.1 C		159.1 C		159.1 C		159.1 C	
9'	87.0 CH	4.58 d (4.0)	87.0 CH	4.60 d (4.0)	87.0 CH	4.58 d (4.0)	86.9 CH	4.59 d (4.2)
10'	29.8 CH	2.86 m	29.8 CH	2.89 m	29.8 CH	2.89 m	29.8 CH	2.86 m
11'	36.1 CH ₂	2.84 m 2.27 m	36.1 CH ₂	2.87 dd (21.6, 9.1) 2.28 dd (21.6, 9.1)	36.1 CH ₂	2.87 dd (21.8, 8.9) 2.26 dd (21.7, 8.8)	36.1 CH ₂	2.86 dd (21.0, 9.3) 2.28 dd (21.5, 9.2)
12'	176.1 C		176.1 C		176.1 C		176.0 C	
13'	20.3 CH ₃	1.15 d (6.4)	20.3 CH ₃	1.17 d (6.5)	20.3 CH ₃	1.15 d (6.6)	20.2 CH ₃	1.15 d (6.3)
14'	169.3 C		169.3 C		169.3 C		169.2 C	
15'	53.9 CH ₃	3.68 s	53.9 CH ₃	3.70 s	53.9 CH ₃	3.68 s	53.9 CH ₃	3.69 s
5'-OH		11.81 s		11.82 s		11.81 s		11.80 s

as H-9 and H-10 to C-8) indicated that the oxidation pattern of C-7 and C-8 in **7** was reversed in **10** (i.e., C-7 bore the hydroxyl group and C-8 was a ketone) (Tables 3 and 4, Figure 2). The

metabolite's absolute configuration was determined to be 7R by comparing experimental ECD data with a theoretical spectrum of the compound (Figure 4B, refer to the Supporting

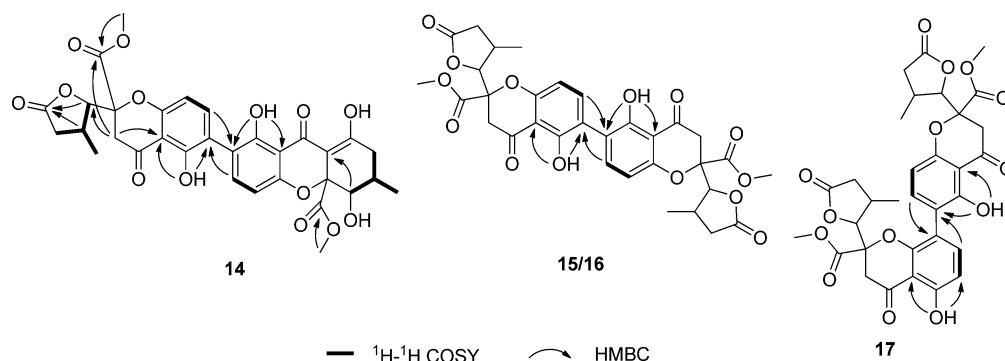


Figure 5. Selected ^1H – ^1H COSY and HMBC correlations for compounds 14–17.

Information for a discussion of how the theoretical ECD data for **10** were prepared). Thus, the structure of the new metabolite was confirmed as illustrated for **10** and was named pyrenochaetic acid G.

The molecular formula of **11** was determined to be $\text{C}_{13}\text{H}_{14}\text{O}_5$ based on HRESIMS, which provided an $[\text{M} - \text{H}]^-$ ion at m/z 249.0776 (calcd 249.0768). A comparison of the 1D NMR data for **11** with **10** (Tables 3 and 4) revealed that the carbon and proton signals attributable to the C-7 methine were missing and had been replaced by a downfield ketone resonance (δ_{C} 196.3). Compound **11** was named pyrenochaetic acid H.

Dimethylamide asterrate (**13**) possessed the molecular formula $\text{C}_{19}\text{H}_{21}\text{NO}_7$ as determined by HRESIMS, indicating that the metabolite possessed 10 degrees of unsaturation. The compound exhibited ^1H and ^{13}C NMR resonances (Table 5) that were similar to the known, co-occurring metabolite asteric acid (**12**),¹⁸ with the major exceptions being the addition of two new methyl groups (C-9': δ_{C} 34.3, δ_{H} 2.91; C-10': δ_{C} 37.5, δ_{H} 2.85). Considering the chemical shift and HMBC correlation data for **13** (δ_{H} 2.91 and 2.85 to δ_{C} 166.2), the new methyl groups were rationalized to be part of a tertiary amide that had replaced the carboxylic acid in **12**.

Compound **14** was obtained as a pale yellow, amorphous solid. On the basis of the HRESIMS data ($[\text{M} + \text{H}]^+$ ion at m/z 639.1708, calcd 639.1714), the molecular formula was established as $\text{C}_{32}\text{H}_{30}\text{O}_{14}$ requiring 18 degrees of unsaturation. Analysis of ^1H NMR, ^{13}C NMR, and HSQC data (Table 6) revealed that this metabolite possessed 17 nonprotonated carbons, eight methines, three methylenes, and four methyl groups. Further analysis of the 2D NMR data (Figure 5) revealed that **14** shared the same planar structure as blennolide G.¹⁹ When the NMR solvent was changed from $\text{DMSO}-d_6$ to CDCl_3 (as reported in the literature), compound **14** provided ^1H and ^{13}C NMR spectra that were identical to blennolide G; however, their specific rotation values were in essence the opposite of one another {**14**: $[\alpha]_{\text{D}}^{25} -68.8$ (c 0.125, CHCl_3); blennolide G: $[\alpha]_{\text{D}}^{25} +81.1$ (c 0.29, CHCl_3)}. Further analysis of the ECD data for **14** (Figure S80) revealed a Cotton effect pattern that was the inverse of that generated for blennolide G. Thus, metabolite **14** was determined to be the antipode of blennolide G.

Like compound **14**, metabolites **15**, **16**, and **17** shared the same molecular formula ($\text{C}_{32}\text{H}_{30}\text{O}_{14}$), as well as many other similarities among their ^1H and ^{13}C NMR spectral data (Table 6). In spite of this, compound **15** stood out as displaying half of the expected proton and carbon resonances, which indicated that it was a symmetrical dimer. HMBC correlation data (Figure 5) were essential for establishing the C-6–C-6' linkage

and overall planar structure of **15**. It was subsequently determined that metabolite **16** shared the same planar structure as **15** (Figure 5). However, the presence of two distinct sets of resonances representing the two monomeric portions of **16** denoted that this metabolite was an asymmetric diastereomer of **15**. In contrast to **15** and **16**, HMBC correlations from H-7' to C-8 and H-7 to C-6' (Figure 5) indicated that metabolite **17** was covalently bonded via a C-8–C-6' linkage. Since compounds **15**–**17** were not active in our panel of assays and were prone to consistent degradation during both freezer storage and room-temperature handling, our investigation of their relative configurations was discontinued.

All the purified compounds were screened for cancer cell cytotoxicity,²⁰ antibacterial²¹ and antifungal²² activities, and inhibition of fungal biofilm formation.⁸ Only compounds **1**–**3** exhibited anti-MRSA activity, with MIC values of 4.1, 4.9, and 3.2 μM (2.9, 3.2, and 2.0 $\mu\text{g/mL}$), respectively, whereas the MIC for chloramphenicol was 5 μM (1.6 $\mu\text{g/mL}$). Metabolites **1**–**3** also showed weak mammalian cell cytotoxicity effects against pancreatic cancer cells (MIA PaCa-2) with IC_{50} values of 50.8, 30.3, and 29.3 μM , respectively.

EXPERIMENTAL SECTION

General Experimental Procedures. UV data were collected on a Hewlett-Packard 8452A diode array spectrophotometer. IR data were collected on a Shimadzu IR Affinity FTIR. Optical rotation data were determined on a Rudolph Research AUTOPOL III automatic polarimeter. NMR data were collected on a Varian 400 MHz NMR instrument. Accurate mass data were collected on an Agilent 6538 HRESI QTOF MS coupled to an Agilent 1290 HPLC. LC-MS data were obtained on a Shimadzu LC-MS 2020 system (ESI quadrupole) coupled to a photodiode array detector, with a Phenomenex Kinetex column (2.6 μm C_{18} column, 100 Å, 75 \times 3.0 mm). The HPLC system utilized SCL-10A VP pumps and a system controller with Luna 5 μm C_{18} columns (110 Å, 250 \times 21.2 mm, 10 mL/min and 110 Å, 250 \times 10 mm, 4 mL/min). X-ray data were collected using a diffractometer with a Bruker APEX CCD area detector and graphite-monochromated Mo K α radiation ($\lambda = 0.71073$ Å). All solvents were of ACS grade or better.

Fungal Isolate Procurement and Culture Conditions. The fungal isolate (internal strain designation Wailua PDA-3) was obtained from a soil sample collected in the vicinity of Wailua Falls, Hawaii. The isolate was identified as similar to *Alternaria longissima* based on ITS sequence analysis (99% sequence homology). Sequence data for the isolate (GenBank accession no. KM088044) was compared by BLAST analysis to sequences publicly available through the NCBI database. The isolate was deposited in our laboratory's fungal library. The fungal isolate was cultured under solid-state conditions on a medium composed of Cheerios breakfast cereal supplemented with a 0.3% sucrose solution with 0.005% chloramphenicol. The fungus was grown for 4 weeks at room temperature (25 °C).

Extraction and Purification. The scale-up solid-phase cultures were pooled and extracted twice overnight with EtOAc, and the organic solvent was partitioned against water. The resultant organic layers were concentrated under vacuum. The resulting extract (71 g) was separated by silica gel VLC (gradient mobile phase consisting of hexane–CH₂Cl₂–MeOH), which yielded four fractions (Fr.1–Fr.4). Fr.2 (eluted with 9:1 MeOH–CH₂Cl₂) was subjected to C₁₈ VLC (H₂O–MeOH) to give four subfractions. Subfraction 1 (eluted with 4:6 H₂O–MeOH) was further purified by semipreparative HPLC (mobile phase 1:1 H₂O–MeOH with 0.1% formic acid in water) to afford compounds **6** (2.0 mg), **7** (15.0 mg), **8** (2.5 mg), **9** (2.8 mg), **10** (3.0 mg), **11** (2.3 mg), and **12** (6.0 mg). Subfraction 3 (eluted with 8:2 H₂O–MeOH) was applied to a Sephadex LH20 column and eluted with 1:1 CH₂Cl₂–MeOH. Further purification by semipreparative HPLC (mobile phase 6:4 to 9:1 MeOH–H₂O with 0.1% formic acid in water) yielded **1** (8.0 mg), **2** (7.5 mg), **4** (25 mg), **5** (14 mg), **13** (6.5 mg), **14** (4.0 mg), **15** (5.1 mg), **16** (4.7 mg), and **17** (5.0 mg).

Polluxochrin (1): pale yellow, amorphous solid; UV (MeOH) λ_{\max} (log ϵ) 210 (4.27), 286 (3.81), 346 (3.54) nm; IR (film) ν_{\max} 3600, 2953, 1712, 1641, 1514, 1454, 1344, 1211, 1091, 1022, 831 cm⁻¹; ¹H and ¹³C NMR see Table 1; HRESIMS [M + Na]⁺ m/z 717.1253 (calcd for C₃₄H₃₀O₁₄SNa, 717.1248).

Dioschirin (2): pale yellow, block-like crystals; UV (MeOH) λ_{\max} (log ϵ) 208 (4.37), 238 (4.34), 364 (4.05) nm; IR (film) ν_{\max} 3600, 2930, 1712, 1645, 1585, 1514, 1365, 1209, 1089, 1020, 831 cm⁻¹; ¹H and ¹³C NMR see Table 2; HRESIMS [M + Na]⁺ m/z 685.0981 (calcd for C₃₃H₂₆O₁₃SNa, 685.0986).

Castochrin (3): pale yellow powder; UV (MeOH) λ_{\max} (log ϵ) 210 (4.39), 246 (4.12), 298 (3.56), 364 (3.90) nm; IR (film) ν_{\max} 3610, 2935, 1739, 1699, 1651, 1514, 1365, 1269, 1211, 1008, 827 cm⁻¹; ¹H and ¹³C NMR see Table S1; HRESIMS [M – H][–] m/z 629.0757 (calcd for C₃₂H₂₁O₁₂S, 629.0754).

Pyrenochaetic acid D (7): colorless cubic crystals; [α]_D²⁵ –5.0 (c 0.18, EtOH); UV (MeOH) λ_{\max} (log ϵ) 212 (4.14), 252 (3.68), 302 (3.32) nm; CD (MeOH) λ_{\max} ($\Delta\epsilon$) 254 (6.82) 317 (–2.50); IR (film) ν_{\max} 2972, 1699, 1541, 1456, 1413, 1315, 1226, 1097, 974 cm⁻¹; ¹H and ¹³C NMR see Tables 3 and 4; HRESIMS [M – H][–] m/z 251.0931 (calcd for C₁₃H₁₅O₅, 251.0925).

Pyrenochaetic acid E (8): colorless, amorphous solid; UV (MeOH) λ_{\max} (log ϵ) 212 (4.12), 246 (3.61), 298 (3.23) nm; IR (film) ν_{\max} 2941, 1697, 1541, 1456, 1413, 1315, 1234, 1095 cm⁻¹; ¹H and ¹³C NMR see Tables 3 and 4; HRESIMS [M – H][–] m/z 251.0931 (calcd for C₁₃H₁₅O₅, 251.0925).

Pyrenochaetic acid F (9): colorless, amorphous solid; UV (MeOH) λ_{\max} (log ϵ) 210 (4.19), 298 (3.34) nm; IR (film) ν_{\max} 2966, 1737, 1687, 1546, 1454, 1413, 1238, 1097, 1039 cm⁻¹; ¹H and ¹³C NMR see Tables 3 and 4; HRESIMS [M – H][–] m/z 293.1034 (calcd for C₁₅H₁₇O₆, 293.1031).

Pyrenochaetic acid G (10): colorless, amorphous solid; [α]_D²⁵ –11.4 (c 0.18, MeOH); UV (MeOH) λ_{\max} (log ϵ) 216 (4.20), 248 (3.79), 296 (3.37) nm; CD (MeOH) λ_{\max} ($\Delta\epsilon$) 244 (6.48), 275 (–1.85); IR (film) ν_{\max} 2965, 1699, 1577, 1456, 1413, 1313, 1226, 1091 cm⁻¹; ¹H and ¹³C NMR see Tables 3 and 4; HRESIMS [M – H][–] m/z 251.0932 (calcd for C₁₃H₁₅O₅, 251.0925).

Pyrenochaetic acid H (11): colorless, amorphous solid; UV (MeOH) λ_{\max} (log ϵ) 212 (4.19), 270 (3.88), 326 (3.46) nm; IR (film) ν_{\max} 2981, 1685, 1548, 1460, 1311, 1255, 1096 cm⁻¹; ¹H and ¹³C NMR see Tables 3 and 4; HRESIMS [M – H][–] m/z 249.0776 (calcd for C₁₃H₁₃O₅, 249.0768).

Dimethylamide asterrate (13): pale yellow, amorphous solid; UV (MeOH) λ_{\max} (log ϵ) 212 (4.33), 284 (3.32), 310 (3.34) nm; IR (film) ν_{\max} 3439, 1625, 1469, 1357, 1249, 1205, 1149, 1060 cm⁻¹; ¹H and ¹³C NMR see Table 5; HRESIMS [M + H]⁺ m/z 376.1392 (calcd for C₁₉H₂₂NO₇, 376.1391).

(–)-Blennolide G (14): pale yellow, amorphous solid; [α]_D²⁵ –68.8 (c 0.125, CHCl₃); UV (MeOH) λ_{\max} (log ϵ): 206 (4.26), 260 (3.97), 340 (3.85) nm; CD (MeOH) λ_{\max} ($\Delta\epsilon$) 211 (8.37), 223 (14.2), 328 (–3.35); IR (film) ν_{\max} 2967, 1788, 1739, 1612, 1435, 1361, 1213,

1047 cm⁻¹; ¹H and ¹³C NMR see Table 6; HRESIMS [M + H]⁺ m/z 639.1708 (calcd for C₃₂H₃₁O₁₄, 639.1714).

Blennolide H (15): pale yellow, amorphous solid; [α]_D²⁵ –75.3 (c 0.473, CHCl₃); UV (MeOH) λ_{\max} (log ϵ) 208 (4.36), 258 (4.30), 364 (3.84) nm; IR (film) ν_{\max} 3439, 2965, 1788, 1645, 1433, 1359, 1273, 1207, 1056 cm⁻¹; ¹H and ¹³C NMR see Table 6; HRESIMS [M + Na]⁺ m/z 661.1530 (calcd for C₃₂H₃₀O₁₄Na, 661.1528).

Blennolide I (16): pale yellow, amorphous solid; [α]_D²⁵ –35.0 (c 0.035, CHCl₃); UV (MeOH) λ_{\max} (log ϵ) 206 (4.32), 256 (4.25), 360 (3.79) nm; IR (film) ν_{\max} 3458, 2962, 1791, 1647, 1433, 1359, 1286, 1207, 1012 cm⁻¹; ¹H and ¹³C NMR see Table 6; HRESIMS [M + Na]⁺ m/z 661.1531 (calcd for C₃₂H₃₀O₁₄Na, 661.1528).

Blennolide J (17): pale yellow, amorphous solid; [α]_D²⁵ –28.8 (c 0.125, CHCl₃); UV (MeOH) λ_{\max} (log ϵ) 210 (4.50), 256 (4.43), 360 (3.93) nm; IR (film) ν_{\max} 3441, 1788, 1745, 1647, 1469, 1354, 1280, 1172, 1055 cm⁻¹; ¹H and ¹³C NMR see Table 6; HRESIMS [M + Na]⁺ m/z 661.1527 (calcd for C₃₂H₃₀O₁₄Na, 661.1528).

X-ray Crystal Structure Analysis of 2 and 7. A yellow plate-shaped crystal of dimensions 0.46 × 0.26 × 0.08 mm of **2** and a colorless prism-shaped crystal of dimensions 0.44 × 0.32 × 0.18 mm of **7** were selected for structural analysis. Intensity data for these two compounds were collected using a diffractometer with a Bruker APEX ccd area detector and graphite-monochromated Mo K radiation (0.710 73 Å). Details of the X-ray crystal structure analysis for **2** and **7** are available in the Supporting Information. The X-ray crystallographic data for **2** and **7** have been deposited with the Cambridge Crystallographic Data Center under accession numbers CCDC 993668 and 993669, respectively. These data can be accessed free of charge at <http://www.ccdc.cam.ac.uk/>.

ECD Calculation Details of 7 and 10. Conformational analyses were carried out using Spartan'10.²³ Geometry, frequency, and ECD calculations were applied at the DFT level with Gaussian 09.²⁴ SpecDis 1.60 was used to average single ECD or UV–vis spectra after Boltzmann statistical weighting.²⁵

Cytotoxicity Assay. Mammalian cell cytotoxicity assays were performed on pancreatic cancer (MIA PaCa-2) cells by adding 5000 cells per well into 96-well plates. The cells were allowed to adhere overnight at 37 °C in a humidified incubator (5% CO₂ atmosphere). Test compounds were diluted in DMSO and added to the wells so that the final concentration of DMSO per well did not exceed 1% by volume. The plates containing treated and control cells were incubated for 48 h, and cell viability was determined by MTT assay.²⁶

Antibacterial Assay. Compounds were tested against methicillin-resistant *Staphylococcus aureus* (MRSA) strain ATCC 700787, which also exhibits reduced susceptibility to vancomycin. A stock culture was diluted in brain heart infusion broth and delivered into presterilized 96-well plates. Stocks prepared in DMSO were added to each well of the 96-well plate (1% final DMSO concentration). Optical density measurements (OD₆₀₀) of the cultures were determined on a Tecan Infinite M200 plate reader. The plates were incubated for 17 h in a humidified incubator at 37 °C. Plates were removed and orbitally shaken, and a final OD₆₀₀ value was recorded. The final OD₆₀₀ reading was subtracted from the initial OD₆₀₀ reading to obtain the change in OD₆₀₀ (antimicrobial activity was determined based on the change in optical density).

■ ASSOCIATED CONTENT

Supporting Information

NMR (¹H, ¹³C, ¹H–¹H COSY, HSQC, and HMBC) and HRESIMS data of **1–3**, **7–11**, and **13–17**, X-ray crystal structure analysis for **2** and **7**, ECD data for compound **14**, and detailed analyses of calculated and experimental ECD data for compounds **7** and **10**. This material is available free of charge via the Internet at <http://pubs.acs.org>.

AUTHOR INFORMATION

Corresponding Author

*E-mail: rhcichewicz@ou.edu. Tel: 405-325-6969. Fax: 405-325-6111.

Notes

The authors declare no competing financial interest.

ACKNOWLEDGMENTS

Research reported in this publication was supported by the National Institutes of Health (1R01AI085161), NSF (CHE-0130835), a Challenge Grant from the Office of the Vice President for Research at the University of Oklahoma, and an award through the Shimadzu Equipment Grant Program.

REFERENCES

- (1) Conry, P. J.; Cannarella, R. *Hawaii Statewide Assessment of Forest Conditions and Trends*; Department of Land and Natural Resources, Division of Forestry and Wildlife, Honolulu, HI, 2010; pp 154–178.
- (2) Lowery, P. P. *Ocean and Aquatic Ecosystems - Vol. II - Patterns of Species Richness, Endemism, and Diversification in Oceanic Island Floras*; United Nations Educational, Scientific and Cultural Organization & Encyclopedia of Life Support Systems, 2009; pp 201–220.
- (3) Greshock, T. J.; Grubbs, A. W.; Jiao, P.; Wicklow, D. T.; Gloer, J. B.; Williams, R. M. *Angew. Chem., Int. Ed.* **2008**, *47*, 3573–3577.
- (4) Sy, A. A.; Swenson, D. C.; Gloer, J. B.; Wicklow, D. T. *J. Nat. Prod.* **2008**, *71*, 415–419.
- (5) Shim, S. H.; Swenson, D. C.; Gloer, J. B.; Dowd, P. F.; Wicklow, D. T. *Org. Lett.* **2006**, *8*, 1225–1228.
- (6) Neff, S. A.; Lee, S. U.; Asami, Y.; Ahn, J. S.; Oh, H.; Baltrusaitis, J.; Gloer, J. B.; Wicklow, D. T. *J. Nat. Prod.* **2012**, *75*, 464–472.
- (7) Wu, Q.-X.; Crews, M. S.; Draskovic, M.; Sohn, J.; John, T. A.; Tenney, K.; Valeriote, F. A.; Yao, X.-J.; Bjeldanes, L. F.; Crews, P. *Org. Lett.* **2010**, *12*, 4458–4461.
- (8) Wang, X.; You, J.; King, J. B.; Powell, D. R.; Cichewicz, R. H. *J. Nat. Prod.* **2012**, *75*, 707–715.
- (9) Gereau, A. L.; Branscum, K. M.; King, J. B.; You, J.; Powell, D. R.; Miller, A. N.; Spear, J. R.; Cichewicz, R. H. *Tetrahedron Lett.* **2012**, *53*, 4202–4205.
- (10) Du, L.; King, J. B.; Morrow, B. H.; Shen, J. K.; Miller, A. N.; Cichewicz, R. H. *J. Nat. Prod.* **2012**, *75*, 1819–1823.
- (11) Cai, S.; Du, L.; Gereau, A. L.; King, J. B.; You, J.; Cichewicz, R. H. *Org. Lett.* **2013**, *15*, 4186–4189.
- (12) Lee, H. J.; Lee, J. H.; Hwang, B. Y.; Kim, H. S.; Lee, J. J. *J. Antibiot.* **2002**, *55*, 552–556.
- (13) Wang, F.-W.; Ye, Y.-H.; Ding, H.; Chen, Y.-X.; Tan, R.-X.; Sun, Y.-C. *Chem. Biodiversity* **2010**, *7*, 216–220.
- (14) Hamasaki, T.; Kimura, Y. *Agric. Biol. Chem.* **1983**, *47*, 163–165.
- (15) Zhang, H.; Mao, L.-L.; Qian, P.-T.; Shan, W.-G.; Wang, J.-D.; Bai, H. *J. Asian Nat. Prod. Res.* **2012**, *11*, 1078–1083.
- (16) Hooft, R. W. W.; Straver, L. H.; Spek, A. L. *J. Appl. Crystallogr.* **2008**, *41*, 96–103.
- (17) Sato, H.; Konoma, K.; Sakamura, S. *Agric. Biol. Chem.* **1981**, *45*, 1675–1679.
- (18) Ohashi, H.; Akiyama, H.; Nishikori, K.; Mochizuki, J. *J. Antibiot.* **1992**, *45*, 1684–1685.
- (19) Zhang, W.; Krohn, K.; Zia-U; Flörke, U.; Pescitelli, G.; Bari, L. D.; Antus, S.; Kurtán, T.; Rheinheimer, J.; Draeger, S.; Schulz, B. *Chem.—Eur. J.* **2008**, *14*, 4913–4923.
- (20) Joyner, P. M.; Waters, A. L.; Williams, R. B.; Powell, D. R.; Janakiram, N. B.; Rao, C. V.; Cichewicz, R. H. *J. Nat. Prod.* **2011**, *74*, 857–861.
- (21) Wang, X.; Filho, J. G. S.; Hoover, A. R.; King, J. B.; Ellis, T. K.; Powell, D. R.; Cichewicz, R. H. *J. Nat. Prod.* **2010**, *73*, 942–948.
- (22) Henrikson, J. C.; Ellis, T. K.; King, J. B.; Cichewicz, R. H. *J. Nat. Prod.* **2011**, *74*, 1959–1964.
- (23) Shao, Y.; Molnar, L. F.; Jung, Y.; Kussmann, J.; Ochsenfeld, C.; Brown, S. T.; Gilbert, A. T.; Slipchenko, L. V.; Levchenko, S. V.; O'Neill, D. P.; DiStasio, R. A., Jr.; Lochan, R. C.; Wang, T.; Beran, G. J.; Besley, N. A.; Herbert, J. M.; Lin, C. Y.; Van Voorhis, T.; Chien, S. H.; Sodt, A.; Steele, R. P.; Rassolov, V. A.; Maslen, P. E.; Korambath, P. P.; Adamson, R. D.; Austin, B.; Baker, J.; Byrd, E. F.; Dachsel, H.; Doerksen, R. J.; Dreuw, A.; Dunietz, B. D.; Dutoi, A. D.; Furlani, T. R.; Gwaltney, S. R.; Heyden, A.; Hirata, S.; Hsu, C. P.; Kedziora, G.; Khalliulin, R. Z.; Klunzinger, P.; Lee, A. M.; Lee, M. S.; Liang, W.; Lotan, I.; Nair, N.; Peters, B.; Proynov, E. I.; Pieniazek, P. A.; Rhee, Y. M.; Ritchie, J.; Rosta, E.; Sherrill, C. D.; Simmonett, A. C.; Subotnik, J. E.; Woodcock, H. L., 3rd; Zhang, W.; Bell, A. T.; Chakraborty, A. K.; Chipman, D. M.; Keil, F. J.; Warshel, A.; Hehre, W. J.; Schaefer, H. F., 3rd; Kong, J.; Krylov, A. I.; Gill, P. M.; Head-Gordon, M. *Phys. Chem. Chem. Phys.* **2006**, *8*, 3172–3191.
- (24) Frisch, M. J.; Trucks, G. W.; Schlegel, H. B.; Scuseria, G. E.; Robb, M. A.; Cheeseman, J. R.; Scalmani, G.; Barone, V.; Mennucci, B.; Petersson, G. A.; Nakatsuji, H.; Caricato, M.; Li, X.; Hratchian, H. P.; Izmaylov, A. F.; Bloino, J.; Zheng, G.; Sonnenberg, J. L.; Hada, M.; Ehara, M.; Toyota, K.; Fukuda, R.; Hasegawa, J.; Ishida, M.; Nakajima, T.; Honda, Y.; Kitao, O.; Nakai, H.; Vreven, T.; Montgomery, J. A., Jr.; Peralta, J. E.; Ogliaro, F.; Bearpark, M.; Heyd, J. J.; Brothers, E.; Kudin, K. N.; Staroverov, V. N.; Kobayashi, R.; Normand, J.; Raghavachari, K.; Rendell, A.; Burant, J. C.; Iyengar, S. S.; Tomasi, J.; Cossi, M.; Rega, N.; Millam, J. M.; Klene, M.; Knox, J. E.; Cross, J. B.; Bakken, V.; Adamo, C.; Jaramillo, J.; Gomperts, R.; Stratmann, R. E.; Yazyev, O.; Austin, A. J.; Cammi, R.; Pomelli, C.; Ochterski, J. W.; Martin, R. L.; Morokuma, K.; Zakrzewski, V. G.; Voth, G. A.; Salvador, P.; Dannenberg, J. J.; Dapprich, S.; Daniels, A. D.; Farkas, Ö.; Foresman, J. B.; Ortiz, J. V.; Cioslowski, J.; Fox, D. J. *Gaussian 09*, Revision A.1; Gaussian, Inc.: Wallingford, CT, 2009.
- (25) Bruhn, T.; Schaumlöffel, A.; Hemberger, Y.; Bringmann, G. *SpecDis*, Version 1.60; University of Würzburg: Germany, 2012.
- (26) Hansen, M. B.; Nielsen, S. E.; Berg, K. *J. Immunol. Methods* **1989**, *119*, 203–210.